

New cermet coatings for mid-temperature applications for solar concentrated combine heat and power system

Ewa Wäckelgård^{a*}, Ruben Bartali^b, Riccardo Gerosa^c, Nadhira Laidani^b, Andreas Mattsson^a, Victor Micheli^b, and Barbara Rivolta^c

^a*Division of Solid State Physics, Department of Engineering Sciences, Uppsala University, Uppsala, Sweden*

^b*Renewable Energy and Environmental Technologies, Fondazione Bruno Kessler, Trento, Italy*

^c*Department of Mechanics, Politecnico di Milano, Milan, Italy*

1. Introduction

Solar heating is in many respects a mature technology for domestic hot water and space heating operating at low temperatures, i.e. 50 to 100 °C. Solar heating systems for higher temperatures, such as for electricity generation have still a potential for improving both components and whole systems. There has been a trend during the first decade of the 21st century to invest in large plants for STE (solar thermal electricity) in sun-belt regions in Europe, Asia, US and Australia. Most effort has been put on reducing costs for the concentrating elements (mirrors or lenses), tracking parts and the electricity generation part or heat storage. Less has been done to develop the solar absorbers, the technology so far has mostly been relying on the developments done during 1980th, the pioneering period of solar electricity technology.

This study focuses on new efficient coatings for solar absorbers to be used in STE trough concentrating systems, where the absorber is a stainless steel tube, vacuum encapsulated and located in the focal line of the trough parabolic reflector (or linear fresnel lenses). These systems can operate from 350°C depending on the thermodynamic cycle used for converting heat to electricity.

1.1. Absorbers in concentrated solar collectors for combined heat and power

The development of a new cermet based solar absorber is a part of the FP7 EU project DiGeSPo (Distributed CHP Generation from small size concentrated Solar Power), a modular 1 to 3 kW_e, 3 to 9 kW_{th} micro combined heat and power system for single and domestic dwellings. It integrates a small scale concentrating solar collector module with sixteen collector tubes operating in the range of 300 to 325°C. The system has been set-up for demonstration at ArrowPharma industrial plant in Malta. The development of the absorber coatings for these collectors will be presented in this conference report. The goal was to achieve a solar absorptance of 0.93 in combination with thermal emittance at 350°C of 0.06.

1.2. Previous work

The prevailing type of coating used in mid-temperature applications has been a cermet (ceramic-metal) composite of Mo-Al₂O₃. [1] This coating has recently been improved by replacing the infrared reflector coating with silver, stabilised with thin silicone dioxide layers to prevent degradation. [2] The emittance at 380°C could then be lowered from 0.13 to 0.06, but in combination with a solar absorptance that decreased from 0.96 to 0.94. There is only a few new coating concepts reported for STE applications, a W-Al₂O₃ coating with a solar absorptance of 0.94 and thermal emittance of 0.10 at 400°C. [3] The coating is made by sputtering deposition and is reported to be stable in vacuum during a 30-days test at 580°C. Both Mo-Al₂O₃ and W-Al₂O₃ absorber coatings referred to above, consist of three sub-layers for solar absorption: a base cermet layer of higher metal content on the infrared reflector, an intermediate cermet layer with a lower metal content and on top, an antireflection coating of a pure dielectric material.

1.3. Outline of study

The main steps in this study to optimize a cermet structure using one or two cermet layers are outlined as follows. First absorber coatings were modeled theoretically in order to select feasible materials composition in the cermets, i.e. choice of metal and dielectric component respectively. As the next step the optical constants of the selected cermet components were determined, as we expected a deviation of optical properties of sputter-deposited thin films compared to bulk properties found in literature. A second round of modeling was then performed with these optical constants to derive cermet coating thicknesses and metal contents. After that absorber coatings were deposited according to these parameters from the modeling. A comprehensive article will be published later on all details in the cermet development in the DiGeSPo project. Here we will focus on the main results concerning optical properties, mechanical properties and stability at operation temperatures for the two cermets that was selected as main candidates for being applied in the collectors of the pilot plant at Malta: W-SiO₂ and Nb-TiO₂ cermets. For

both types of absorbers it was used SiO₂ as top antireflection (AR) coating and molybdenum as infrared (IR) reflector.

2. Methods

As mentioned above the study includes both theoretical and experimental parts. The samples went through optical, mechanical and structural characterization before and after temperature tests. In the following we present the routines and instruments for modelling, sputtering-deposition, materials characterization and finally temperature testing.

2.1. Theoretical calculations

Theoretical modeling to optimize the optical performance for the three-layer solar absorber stacks were done with SCOUT software tool for optical simulation and optimization of optical coatings.[4] The program uses the complex refractive index, for each layer to calculate the reflectivity of the total stack of layers. For the cermet layers the Bruggeman effective medium theory is used to model effective optical constants of the cermets.

The key values for evaluating optical performance of solar absorber coatings are the *solar absorptance*,

$$\alpha_{sol} = \frac{\int_{0.3\mu m}^{4.1\mu m} I_s(\lambda)\alpha(\lambda) d\lambda}{\int_{0.3\mu m}^{4\mu m} I_s(\lambda) d\lambda} \quad (1)$$

and *thermal emittance*

$$\varepsilon_T = \frac{\int_{0.3\mu m}^{100\mu m} I_{bb}(\lambda)\varepsilon(\lambda) d\lambda}{\int_{0.3\mu m}^{100\mu m} I_{bb}(\lambda) d\lambda} \quad (2)$$

For solar spectral distribution $I_s(\lambda)$ the ASTM 1.5 spectrum is used and the spectral distribution of blackbody radiation $I_{bb}(\lambda)$, was calculated for 350°C. The spectral absorptance $\alpha(\lambda)$, and emittance, $\varepsilon(\lambda)$ is derived from $I-\rho(\lambda)$, where $\rho(\lambda)$ is theoretically calculated spectral reflectance from SCOUT simulations or experimentally measured reflectance on fabricated samples. We have restricted the integration interval to be the in range of the optical instruments that was used.

2.2. Coating deposition

The Mo-layers, W-SiO₂ cermets layers and SiO₂ AR-layers were prepared in a Balzer UTT400 sputtering unit at Ångström Laboratory Uppsala University. The coatings were deposited using direct current (DC) magnetron-sputtering from a molybdenum target for IR reflector, radio frequency (RF) magnetron co-sputtering from a silicon oxide and tungsten targets for the cermet layers, and AR-layers. The sample holder was rotated to obtain even thickness of deposited layers. The Nb-TiO₂-cermets were prepared in on-site built sputtering unit at Fondazione Bruno Kessler in Trento using a co-sputtering technique. The TiO₂ films were deposited by RF plasma sputtering of a titanium oxide target while Nb was deposited by RF magnetron-sputtering.

Firstly, a set of samples on Corning glass was sputtered in order to determine the optical constants of the constituents in the cermets: W, Nb, SiO₂ and TiO₂. The samples were made semi-transparent in order to measure their reflectance and transmittance. Sample thickness for SiO₂ and W based layers was determined with a Dektak

XT stylus profilometer whereas the TiO₂ and Nb based layers was determined with a KLA Tencor P15T stylus profilometer. Similar sputtering conditions were used when preparing the oxides on glass and in the cermets.

The substrate was electro-polished stainless steel, which was thermally annealed for one hour in air at 100°C to remove stress and then cleaned by ethanol in an ultra sonic bath before deposition.

2.3. Sample characterization

The main characterization of the absorber coatings is based on optical measurements of reflectance within the solar wavelength range for calculation of solar absorptance (Eq 1) and the infrared wavelength range to calculate thermal emittance at 350°C (Eq 2). Additional to this, it is important to investigate materials composition, contamination, adhesion to substrate, layer thicknesses, type of growth and alteration after temperature tests at operation conditions.

A Perkin-Elmer Lambda 900 UV/VIS/NIR double beam spectrophotometer was used for measurements in the solar spectral range from 0.3 to 2.5 μm. The instrument is equipped with an integrating sphere to allow for measurements on optically rough surfaces. A Spectralon sample was used as reference. Measurements were done at near normal angle of incidence. For the samples on glass both reflectance and transmittance were measured. For the infrared wavelength range TENSOR 27 FTIR from Bruker optics was used. It is equipped with an integrating sphere coated with gold. The measuring wavelength range is from 2.5 to 22 μm. Extrapolation to 100 μm was done to cover the far infrared range. Measurements were done at near normal angle of incidence.

Auger electron spectroscopy (AES) was carried out using a Physical Electronics model 4200 system, equipped with a variable resolution cylindrical mirror analyzer and a coaxial electron gun. WKLL, CKLL, SiLMM and OKLL Auger lines were acquired in derivative mode. Three types of analysis were performed: survey scan spectra of the surface of the as-received samples, survey scan spectra after 1 min of ion etching and multiplex of metal region after 1 min of ion etching.

Grazing incidence X-ray diffraction (XRD) was performed with a Siemens D5000 instrument, equipped with a Goebel mirror to filter out the CuKα radiation. For these measurements the films were deposited directly on amorphous glass substrates (Corning glass) to prevent strong signals from the metals in the stainless steel and Mo infrared reflector.

The scanning Electron Microscope (SEM) used in this study was a Zeiss EVO 50, with 30kV maximum acceleration voltage, 5-150 000 times magnification, equipped with an Oxford EDXS analyser. The observations were carried out directly on the coatings and after a cross sectioning. The cross sections were mounted and polished before the observations.

Scratch tests were performed according to ASTM C 1624-05 Standard both before and after annealing at 350°C under vacuum. According to the standard, tests can be carried out both with constant loads or with increasing loads during the indenter stroke. The indenter is a Rockwell C diamond cone with tip angle and radius respectively equal to 120° and 200 μm. In the present investigation an increasing load technique has been employed, according to the following parameters: scratch length 3 mm, translation speed 1.25 mm/min and maximum load 30 N.

2.4. Durability tests at 350°C

Annealing was made in a pipe oven. A gauge meter was installed at one end of the tube chamber and a pressure of $5 \cdot 10^{-5}$ mbar could be reached. If not indicated the annealing time was first 72 h (3 days), then optical measurement were performed and the annealing continued up to totally 1500 h and the samples were optically re-measured.

3. Results and discussion

The optical performance of modeled and deposited samples is compared. Material characterization supports that there is a real metal and oxide composite (cermet) in both types of absorbers. Mechanical characterization shows a good adhesion of coatings to substrate. Finally temperature test show stability of the coatings at operational temperatures.

3.1. Optical performance of absorber coatings

Table 1 below shows the results from optimized modelled and best results for real sputter-deposited absorbers. The modelled coatings using optical constants for bulk materials gives the best optical performance with respect to the combination highest absorptance/lowest thermal emittance for both cermet types. However the absorber with W-SiO₂ cermet has a higher solar absorptance than the Nb-TiO₂ cermet. Using optical constants derived from the sputter-deposited samples, the two modeled absorbers gets an increase in emittance. Comparing with the sputter-deposited absorber coatings the W-SiO₂ cermet absorber has a lower absorptance and also lower emittance than the modelled absorber using optical constants from sputter-deposited films. The sputter-deposited Nb-TiO₂ cermet absorber shows the same performance as the modeled coating with optical constants from sputter-deposited films. The reason why modeled real coatings gives different optimal results is probably complex and includes as one reason a too simple effective medium model, difficulties to obtain accurate optical constants from reflectance and transmittance measurements of thin films, a third reason is the cermet structure, which will be discussed in the next section.

Table 1. Comparison of results from optimisation: theoretical with literature optical constant, theoretical using optical constants from sputtered samples, and experimentally, in sputter-deposited coatings. Thicknesses of sputter-deposited coatings are determined from TEM.

| | α_{sol} | e_{350} | Base layer (cermet) | | Middle layer (cermet) | | AR layer t_3 (nm) |
|---|----------------|-----------|---------------------|------------|-----------------------|------------|------------------------|
| | | | f_1 | t_1 (nm) | f_2 | t_2 (nm) | |
| SiO₂/W-SiO₂/Mo/SS | | | | | | | |
| Modelled coating and Mo layer with optical constants for bulk materials [4,5] | 0.93 | 0.06 | 0.45 | 70 | 0.20 | 65 | 75 |
| Modelled coating with optical constants from the sputtered films | 0.93 | 0.09 | 0.33 | 75 | 0.08 | 42 | 51 |
| Sputtered coating | 0.91 | 0.08 | | 60 -65 | | 48 | 80-85 |
| SiO₂/Nb-TiO₂/Mo/SS | | | | | | | |
| Modelled coating and Mo layer with optical constants for bulk materials [4,6] | 0.90 | 0.06 | 0.55 | 45 | 0.05 | 25 | 85 |
| Modelled coating with optical constants from the sputtered films | 0.93 | 0.09 | 0.79 | 47 | 0.25 | 29 | 79 |
| Sputtered coating | 0.93 | 0.09 | | 20 | | 50 | 70 |

The spectral reflectance comparing the three cases for the W-SiO₂ cermet absorber in Table 1 is presented in Fig.1 below. It is notable that the infrared reflectance is higher when bulk optical constants are used and the reflectance is lower over a wider spectral range in the solar range.

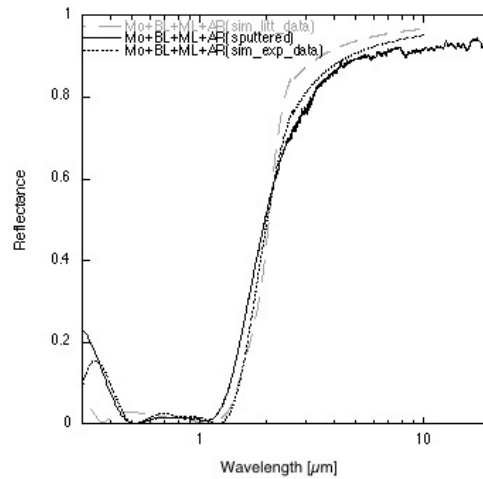


Fig. 1. W-SiO₂ optimised solar absorber with molybdenum IR reflector on stainless steel, W-SiO₂ base layer (BL), W-SiO₂ (ML) and SiO₂ AR layer. Optical constants from literature and derived from sputtered films of W and SiO₂ are used in the two modelled absorbers.

3.2. Cermet characterization from XRD and AES

The function of the cermet is to provide high absorption in very thin coating from the metal component. That means that the particles must be of good metallic quality. Results from XRD and AES shows that the base layer coating has W and Nb in metal phase in the two types of cermet. From XRD the particle size for both W and Nb could be estimated to be about 3 nm using the Debye Sherrer formula. From transmission electron microscopy (TEM) it was not possible to distinguish tungsten particles from silica particles. Both base and middle layer has the same appearance of about 2 nm grains without any ordering from observable atomic planes. For Nb-TiO₂ it is observed distinguishable Nb particles in the size of 5 to 10 nm. The difference in structure between the two cermet types can be an effect of materials dependent sputtering conditions but that is not possible to confirm because two different sputter units has been used for the two coatings, which can be more important for the actual results. More details from the TEM study will be presented in a comprehensive report.

The oxide matrices, SiO₂ and TiO₂ respectively, were not detectable in XRD which then indicates an amorphous structure or sub-nano sized grains for the oxide component in the cermets. This is usually the case when the coatings are deposited without heating the sample holder. ERDA (Elastic Recoil Detectio Analysis) results indicate that the oxides have a 1:2 relation between Si and Ti respectively to oxygen. These results support cermets structures with distinguishable metal particles and oxides. More detailed results from ERDA will be presented in a comprehensive report.

The cermet characterizations confirm a metal phase that is the origin to the solar absorption. It also indicates that the better optical performance for the Nb-TiO₂ cermet absorber can originate from more well define metal particles (visible in TEM) than in the case of the W-SiO₂ cermet absorber. This can be the reason for a better optical performance of the Nb-TiO₂ cermet absorber.

3.3. Mechanical properties from electron microscopy and scratch tests

SEM top views reveals a smooth surface without cracks, where the main topology of parallel horizontal scratch lines originates from the rolling of the stainless steel in manufacturing. Fig. 2 shows the absorber layer stack between the stainless substrate and the embedding resin used for the polishing. From the observation it seems that the adhesion of the coating to the substrate is good.

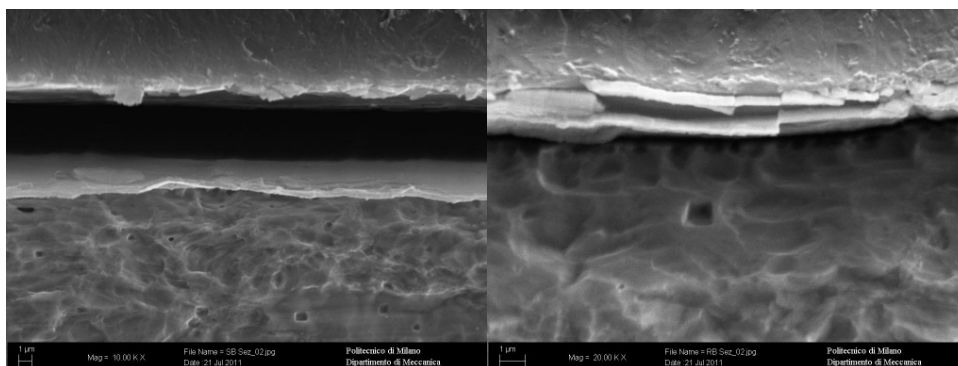


Fig. 2. Cross sectional view of W-SiO₂ absorber (left) and Nb-TiO₂ absorber (right).

Among the scratch testing machine available results, the tangential force and the drag coefficient have been selected as the most interesting for the present analysis. The scratch tests revealed that the coatings mechanical strengths are generally satisfying, and after annealing their behaviour seems to even improve, see Fig. 3.

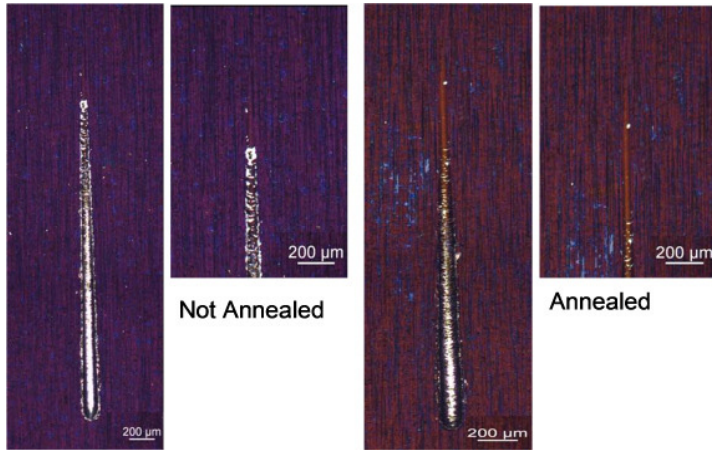


Fig. 3. Scratches performed on W- SiO₂ before and after annealing

3.4. Durability tests at 350°C

There is a small change in the reflectance due to the annealing that primarily influences the thin film interference pattern and implies a change in thickness and/or materials composition in at least one layer. The change takes place during the first test period of 72 hours, after that the solar absorptance and thermal emittance are stable. Fig. 4 shows the spectral reflectance before and after annealing of the Nb-TiO₂ cermet absorber. The absorptance is not changed but the emittance is decreased with 0.01 units for both types of absorbers.

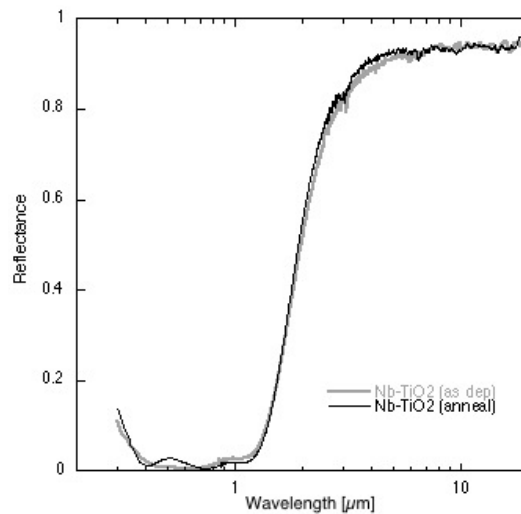


Fig. 4. Reflectance before and after annealing at 350 °C in vacuum for Nb-TiO₂.

4. Conclusions

The aim of this study was to develop a solar-absorbing coating using cermet layers in order to obtain high solar absorption. The procedure was to first model coatings using optical constants from bulk materials in order to select cermet candidates for which a solar absorptance of 0.93 in combination with thermal emittance 0.06 at 350°C could be achieved. The two selected cermets, W-SiO₂ and Nb-TiO₂, were then in a second step modeled with optical constants determined from sputter-deposited thin films and as a third step these model parameters were used to deposit absorber coatings. The results show that the W-SiO₂ cermet absorber cannot reach the 0.93/0.06 performance for the real samples, only when modeled with bulk data. The Nb-TiO₂ cermet absorber does not reach this performance neither for the modeled absorber nor for the real sample, but the real sample has in this case a better performance than the modeled using bulk data. Even though there are differences in performance between modeled and real absorbers these are small and we conclude that the modeling with effective medium models of cermet layers can be used in an optimization procedural.

Coating adherence is found to be good from mechanical testing as well as stability at operational temperatures and even improved after annealing. In a next step up-scaling to deposition on tubes has been made for the Nb-TiO₂ cermet type coating and such absorbers are now operating in the solar concentrating combined heat and power demonstration plant in Malta.

Acknowledgements

The EU FP7 is acknowledged for funding the study as a part of the FP7 EU project DiGeSPo.

Daniel Primetzhofer and Fredrik Gustavsson, Ångström Laboratory are acknowledged for contributing with ERDA measurements and TEM studies that are only briefly presented in this report.

References

- [1] Lanxner M, Elgat Z. Proc. Soc. Photo-Opt. Instr. Eng. 1272 (1990).
- [2] Hildebrandt C. in Fakultät Energie-, Verfahrens- und Biotechnik (Universität Stuttgart, Stuttgart, 2009), Doctoral thesis.
- [3] Antonaia A, Castaldo A, Addonizio M L, et al. Solar Energy Materials & Solar Cells (2010).
- [4] Theiss W. Hard and Software for Optical Spectroscopy, Aachen, Germany. 2002.
- [5] Palik E D. Handbook of Optical Constants of Solids, Academic Press San Diego (1998).
- [6] Weaver J H, Lynch D W, Olson C. G. Phys. Rev. B. 7 p. 4311 (1973).